

Novel Hierarchic Structures in Polymer Blends

Gavin A. Buxton,* Nigel Clarke

Summary: We use computer simulations to investigate the dissolution and phase separation process in polymer blends. In particular, we take initial cylindrical and spherical structures and allow them to dissolve in the one phase region. Before the structure can completely dissolve, however, we thrust the system into the two-phase region. Phase separation then occurs such that hierarchic structures are formed both inside and outside the confines of the original structure. These novel hierarchic structures can be of significant technological importance.

Keywords: blends; dissolution; microstructure; phase separation; simulations

Introduction

Blending polymers is an attractive way of combining the physical characteristics of two different polymers in a single material [1]. However, the macroscopic properties of polymer blends are often found to be sensitive to their internal structure. Typically, a polymer blend is immiscible and phase separation will result in either a dispersed or bicontinuous morphology. Dispersed morphology refers to droplets of one polymer inside a matrix of the other polymer, while bicontinuous morphology refers to both phases interpenetrating in such a way that they both percolate throughout the material. However, the internal structure of polymer blends can be considerably more complex, and in order to enhance macroscopic properties it is necessary to exhibit some control over the microscopic morphology.

An interesting, and relatively simple, way of influencing a polymer blend morphology is to vary the thermodynamic parameters with time [2–6]. An early example of this technique was the work of Onuki et al. [2,3] who investigated the competition between phase separation and dissolution by periodically varying the temperature such that the system alternated between the

one- and two-phase regions. Another, more popular, example of phase separation under time-dependent thermodynamic conditions involves subjecting the system to a “double quench” [7–10]. Generally, this refers to when a system is allowed to phase separate at a shallow quench before being thrust into a second, much deeper, quench. Subsequent to the first quench large shallow domains begin to form. The second quench then causes further phase separation *inside* these domains to form hierarchic structures consisting of large domains containing dispersed microdomains.

An alternative route to creating hierarchic structures is to take systems with pre-existing structure and subject them to a dissolution and phase separation process [4–6]. We first allow the system to *partially* dissolve in the one-phase region before thrusting it into the two-phase region. That is, complete dissolution does not occur and the initial structure is partially preserved. Therefore, some history of the original structure remains and phase separation now occurs both outside and *inside* the confines of the initial structure. It is this complex dissolution and phase separation process which will be the focus of this work. In particular, we are interested in the structures that emerge from pre-existing cylindrical and spherical domains.

In section 2 we detail the Flory-Huggins Cahn-Hilliard method used to elucidate the

Department of Chemistry, University of Durham, Durham, DH1 3LE, United Kingdom

phase separation dynamics in polymer blends. Results are presented in section 3 which depict the novel hierarchic structures that can emerge from the dissolution and phase separation process. Finally, in section 4 we summarise our investigation and draw relevant conclusions.

Computer Simulations

Computer simulations enable us to visualise the phase separation process in polymer blends in minute detail. For example, we can stop the simulation at any moment of time and know exactly what the polymer concentration and flux is at any point in space. It is this detailed insight into the physical mechanisms of phase separation which makes computer simulations so useful. Material parameters and processing conditions can also be systematically varied with relative ease in computer simulations, enabling us to predict new and more interesting behaviour in these complex systems.

The simulation technique we use throughout this study is the Flory-Huggins Cahn-Hilliard model. Three-dimensional systems are considered of size $100 \times 100 \times 100$ and the systems possess periodic boundary conditions in all three directions. The polymer blend is described in terms of the local concentration of polymer A, ϕ ; the concentration of polymer B is given by $(1 - \phi)$, due to incompressibility constraints. For simplicity, we restrict the current study to symmetric polymer blends in which the degree of polymerisation is the same for both the A and B polymers, $N = 2000$. The kinetic equation describing the evolution of the system is given by [11–13]

$$\frac{\partial \phi}{\partial \tau} = \nabla \cdot M(\phi) \nabla \frac{\partial F}{\partial \phi} \quad (1)$$

where $M(\phi)$ represents the polymer mobility and $F \equiv F\{\phi(r, t)\}$ is the free energy functional which consists of both local and gradient contributions [14]. The mobility of a polymer species is assumed to be proportional to its concentration, resulting in a concentration dependent mobility of the form, $M(\phi) = D\phi(1 - \phi)^{[15,16]}$.

As mentioned earlier, the free energy functional is composed of both local and gradient contributions; the former dictates the local entropy of mixing, while the latter introduces a surface tension which drives domain coarsening. The local contribution to the free energy is taken from the Flory-Huggins theory and is given by

$$\frac{F_{FH}}{k_B T} = \int_V \frac{\phi}{N_A} \ln \phi + \frac{1 - \phi}{N_B} \ln(1 - \phi) + \chi \phi(1 - \phi) dr \quad (2)$$

where k_B is the Boltzmann constant, T is the temperature and χ is the enthalpic interaction parameter [17,18]. The integration is over the volume of the system.

The gradient contribution to the free energy is given by [13,15]

$$\frac{F_{dG}}{k_B T} = \int_V \frac{1}{36} \left[\frac{l_A^2}{\phi} + \frac{l_B^2}{1 - \phi} \right] |\nabla \phi|^2 dr \quad (3)$$

where l_i is the Kuhn length of species i , which we take to be the same for both polymers ($l_A = l_B = l$). Substituting Equations 2 and 3 into Equation 1 results in the following dimensionless (and appropriately scaled) evolution equation [5,6,13]

$$\begin{aligned} \frac{\partial \phi(\mathbf{x}, \tau)}{\partial \tau} = & \nabla \cdot \phi(1 - \phi) \nabla \\ & \times \left[\frac{1}{N|\chi_m - \chi_s|} \ln \frac{\phi}{1 - \phi} - \frac{2\chi\phi}{|\chi_m - \chi_s|} \right. \\ & \left. + \frac{2\phi - 1}{36\phi^2(1 - \phi)^2} (\nabla \phi)^2 - \frac{\nabla^2 \phi}{18\phi(1 - \phi)} \right] \end{aligned} \quad (4)$$

where $\tau = D(\chi_m - \chi_s)^2 t / l^2$ represents the dimensionless time scale and \mathbf{x} the dimensionless length scale. χ_m is the maximum χ value used during the simulation (the deepest quench) and χ_s the value of χ at which phase separation occurs. It is straight forward to solve equation 4 using the finite difference method (see Glotzer [13] for details). A time step of $\Delta \tau = 0.02$ and a spatial discretization of $\Delta x = 1/\sqrt{8}$ are used in the current study, although these values were varied to ensure that the results were not an artifact of the discretization. This model allows us to simulate the kinetics of

both the dissolution of the pre-existing structure and the subsequent phase separation from the partially dissolved morphology in a computationally efficient manner.

Results

We first turn our attention to the evolution of a polymer blend containing a cylindrical phase undergoing a dissolution and phase separation process. Figure 1 shows a series of snapshots which depict this process as a function of time. The initial structure is a cylindrical tube with a radius of $20 \Delta x$ and the snapshots depict cross-sectional concentration profiles. Figure 1A shows the initial cylindrical structure as a circle of A polymer inside a matrix of B polymer. Subsequent to dissolution, at $\chi = 0.0001$ for $2000 \Delta t$, the structure is no longer well defined (Figure 1B). Instead, the structure has been allowed to diffuse out resulting in a region of slightly higher concentration with a large and diffuse interphase. Before the structure is completely dissolved, however, the system is thrust into the two-phase region resulting in the phase separation process depicted in Figures 1C to 1F.

Initially, concentric rings are formed which grow in magnitude as the system comes out of partial solution. The outer rings become unstable and phase separation occurs which causes distinct domains to be formed around the structure. Finally the inner ring collapses to form a single column resulting in the structure shown in Figure 1F.

A better view of this structure can be seen in Figure 2 which shows an isosurface plot of the same system, but at a time of $\tau = 3500 \Delta \tau$. Only half of the system is depicted for clarity and the inner column can be clearly seen along with the outer rings of first B polymer and then A polymer. The central A polymer column, in other words, is completely surrounded by B polymer, which is itself completely surrounded by a cylindrical shell of A polymer. In the B polymer matrix, near to this cylindrical hierarchic structure, the outer ring (as shown in Figure 1C) has become unstable and resulted in the formation of highly elongated droplets in the x-direction. Therefore, through the use of a dissolution and phase separation process we can take a simple cylindrical geometry and create a relatively complex morphology.

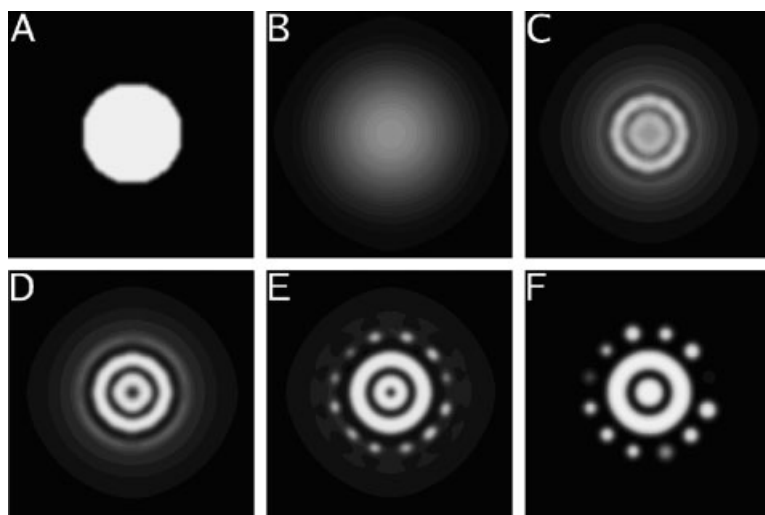


Figure 1.

Dissolution and phase separation process. Contour slice through 3D cylindrical system at time A) $\tau = 0$, B) $\tau = 2000 \Delta \tau$, C) $\tau = 2500 \Delta \tau$, D) $\tau = 2600 \Delta \tau$, E) $\tau = 3000 \Delta \tau$, and F) $\tau = 4000 \Delta \tau$.

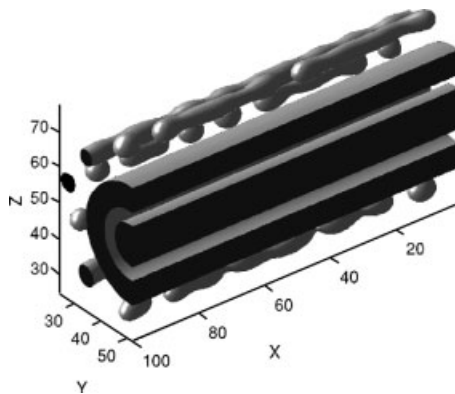


Figure 2.

Cylindrical system subject to dissolution and phase separation process. $\tau = 3500\Delta\tau$. Isosurface separates A-rich from B-rich domains, and the B domains are transparent.

We now consider the dissolution and phase separation process when applied to spherical droplets. Figure 3 shows a series of snapshots detailing the phase separation process in a system which initially contained a spherical particle; the figures depict contour plots of the concentration as slices through the 3D system. The spherical droplet initially has a radius of $25\Delta x$ and the system is allowed to dissolve for $2000\Delta t$ prior to being thrust in to the two-phase region.

Figure 3a shows the system at time $\tau = 2500\Delta\tau$ where the partially dissolved structure has phase separated to form concentric spheres. Subject to further phase separation the system begins to form more well-defined domains. Finally, the morphology consists of the hierarchic structure depicted in Figure 3d. There exists a small droplet of A polymer in the centre of where the initial droplet lay, surrounded by spherical shells of both B polymer and A polymer. Again, we see the formation of droplets in the B polymer matrix, near to this structure.

It is interesting to observe the effects of this dissolution and phase separation process on droplets of different sizes. Figure 4 depicts the morphologies from systems which initially contained droplets of different sizes (radii of $20\Delta x$, $25\Delta x$, and $30\Delta x$).

For the system that initially contained the smallest droplet the resulting spherical structure consists simply of a droplet of B polymer encased in a shell of A polymer. However, as the size of the initial droplet is increased the formation of increasingly complex concentric patterns is observed. In particular, the third system forms a particulate of A polymer, which contains microdomains of B polymer, surrounded by concentric shells of both B and A polymer. This structure is surrounded by a random dispersion of A polymer droplets in the B polymer matrix.

Conclusions

We have highlighted the ability of computer simulations to investigate the formation of hierarchic structures in polymer blends subject to a dissolution and phase separation procedure. In particular, we emphasise the predictive capabilities of computer simulations by investigating the consequences of dissolution and subsequent phase separation on initial cylindrical and spherical structures.

We find that the cylindrical system can form a complex structure consisting of a central column of A polymer surrounded by rings of both B and A polymer, respectively. This geometry curiously resembles a biaxial cable which consists of a central wire and shielding “mesh” separated by an insulating layer. One might imagine that if the A polymer was conductive, or contained conductive particles, then this structure could serve an electronic purpose. Furthermore, following the dissolution and phase separation of droplets we observe the formation of interesting spherically-symmetric structures. For a relatively small initial droplet size we find that the emergent structure consists of a droplet of B polymer encased in a shell of A polymer. Such micro-encapsulation of one polymer within another can be potentially useful in a wide range of scientific areas: with applications ranging from drug delivery^[19] to fracture mechanics^[20].

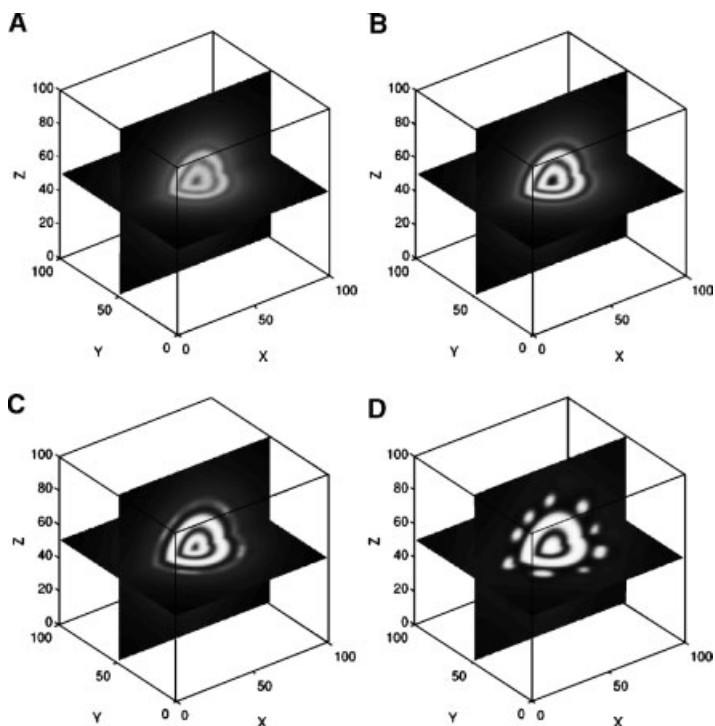


Figure 3.

Contour slices through 3D spherical system (radius = $25 \Delta x$) at time A) $\tau = 2500 \Delta \tau$, B) $\tau = 2600 \Delta \tau$, C) $\tau = 3000 \Delta \tau$, and D) $\tau = 4000 \Delta \tau$.

We have, therefore, shown how using computer simulations we can predict potentially useful polymer blend morphologies. It is through the manipulation of these morphologies that new and more interesting applications for polymer blends

can be realised. We believe that future work should further explore the formation of these structures (along with methods of stabilising these transient morphologies) and seek to validate these predictions through commensurate experimental studies.

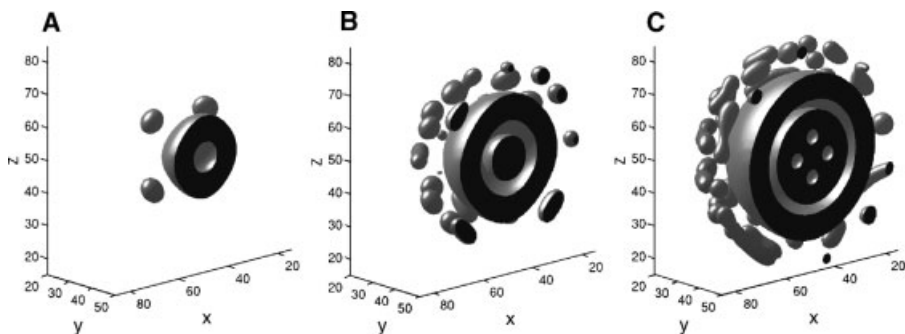


Figure 4.

Effects of dissolution and phase separating process on spheres of size A) $20 \Delta x$, B) $25 \Delta x$, and C) $30 \Delta x$. Isosurfaces separate A-rich from B-rich domains, and the B domains are transparent.

- [1] D.R. Paul, C.B. Bucknall, "Polymer Blends", Wiley, New York 2000.
- [2] A. Onuki, *Phys. Rev. Lett.* **1982**, 48, 753.
- [3] M. Joshua, W.I. Goldburg, A. Onuki, *Phys. Rev. Lett.* **1985**, 54, 1175.
- [4] M. Graca, S.A. Wieczorek, R. Holyst, *Macromolecules* **2002**, 35, 7718.
- [5] N. Clarke, *Phys. Rev. Lett.* **2002**, 89, 215506.
- [6] G.A. Buxton and N. Clarke, *Phys. Rev. E* **2005**, 72, 011807.
- [7] H. Tanaka, *Phys. Rev. E* **1993**, 47, 2946.
- [8] J. Tao, M. Okada, T. Nose and T. Chiba, *Polymer* **1995**, 36, 3909.
- [9] T. Sigehuzi and H. Tanaka, *Phys. Rev. E* **2004**, 70, 051504.
- [10] I.C. Henderson and N. Clarke, *Macromolecules* **2004**, 37, 1952.
- [11] J.W. Cahn and J.E. Hilliard, *J. Chem. Phys.* **1958**, 28, 258.
- [12] J.W. Cahn, *J. Chem. Phys.* **1965**, 42, 93.
- [13] S.C. Glotzer, *Annu. Rev. Comput. Phys.* **1995**, 2, 1.
- [14] The 'Cookean' noise term is neglected from the current study. This term, however, has been found to have little effect on the domain growth of simple fluids and is often omitted from polymeric studies for computational reasons. See Glotzer (Reference 13) for more details.
- [15] P.G. deGennes, *J. Chem. Phys.* **1980**, 72, 4756.
- [16] F. Brochard, J. Jouffroy, and P. Levinson, *Macromolecules* **1983**, 16, 1638.
- [17] P.J. Flory, "Principles of Polymer Chemistry", Cornell University press, New York 1953.
- [18] M.L. Huggins, *J. Am. Chem. Soc.* **1942**, 64, 1712.
- [19] T. Kato, K. Sato, R. Sasaki, H. Kakinumi, and M. Moriyama, *Cancer Chemother. Pharmacol.* **1996**, 37, 289.
- [20] S.R. White et al., *Nature* **2001**, 409, 794.